Environmental Science: Atmospheres

PAPER

Cite this: *Environ. Sci.: Atmos.*, 2022, **2**, 1438

Unraveling the interaction of urban emission plumes and marine breezes involved in the formation of summertime coastal high ozone on Long Island†

Jie Zhang,*[a] Alexandra Catena,[a] Bhupal Shrestha,[b] Jeffrey Freedman,[a] Elizabeth McCabe,[a] Margaret J. Schwab,[a] Dirk Felton,[c] John Kent,[c] Bob Gaza[c] and James J. Schwab*[a]

The New York City (NYC) urban region and locations downwind (*i.e.*, Long Island) are currently characterized as one of the critical regions for studying ozone pollution with special emphasis on the interplay of the urban plume and marine breeze on warm summer days. We use the data from a new air quality monitoring site at the Long Island south shore to provide a contrast to the existing measurements along the north shore and middle of the island. We find different mechanisms for high ozone cases at the north shore *vs.* those resulting in high ozone at the south shore. The north shore high ozone cases mainly result from (1) a calm condition favoring high ozone formation over NYC urban regions and western Long Island, (2) a sea-breeze front originating from south Long Island diverting the high ozone plume to the north shore, and (3) the stagnation of the sea-breeze front over the Long Island north shore (and coastal Connecticut) for several hours. The cases with higher elevated ozone on the south shore are rarely reported due to the limited measurements and are highlighted in this study. They resulted from more varied wind flow patterns, but in each case involved westerly or southwesterly flow and polluted air transported to the site over the ocean in the late afternoon (around 17:00 local time). Different from the previous studies over other regions in the world where the high ozone area generally happened further inland following the sea breeze front movement, the narrow high ozone band mainly covering Long Island south coastal line can be more harmful to the clustered people enjoying the summer beach. This study highlights the necessity of setting up more air quality monitors sites along the Long Island south shore and provides guidance for other shore regions for focusing on the potential for narrow high ozone bands concentrated over near coastal areas.

Received 31st May 2022
Accepted 7th September 2022

DOI: 10.1039/d2ea00061j

rsc.li/esatmospheres

Environmental significance

Ground-level ozone pollution remains a stubborn problem for many cities and downwind locations, including NYC, Long Island, and coastal Connecticut. As a secondary pollutant, ozone is formed from the combination of precursor emissions, most rapidly under warm temperatures, and high solar insolation. Ozone is often most efficiently formed somewhat downwind from the source of the precursor emissions, and high ozone concentrations are carried further downwind by prevailing winds before being diluted to lower levels. This study explores the complicated formation and transport dynamics downwind of NYC on Long Island, where the circulation is also influenced by sea-breeze, shore-breeze, low-level jet, and other more local circulation patterns. Measurements with a high spatial resolution are required to fully explain this complex situation.

1. Introduction

Despite the reduction of emissions of anthropogenic pollutants as tracked by inventories,[1–6] the New York City (NYC) urban region and locations downwind (*i.e.*, Long Island and southern Connecticut (CT)) continue to suffer summertime ozone (O_3) exceedance issues,[7] which has caused much concern for regulators, policymakers, and residents. To help address knowledge and data gaps associated with this problem, the 2018 Long Island Sound Tropospheric Ozone Study (LISTOS, **https://**

[a]Atmospheric Sciences Research Center, University at Albany, State University of New York, Albany, NY, USA. E-mail: jschwab@albany.edu; jzhang35@albany.edu
[b]NYS Mesonet and Atmospheric Sciences Research Center, University at Albany, State University of New York, Albany, NY, USA
[c]Division of Air Resources, New York State Department of Environmental Conservation, Albany, NY, USA

† Electronic supplementary information (ESI) available. See **https://doi.org/10.1039/d2ea00061j**

www.nescaum.org/documents/listos) was established to help explore the evolving nature of summertime O_3 formation and transport in the NYC urban region and locations downwind. In addition to LISTOS in the NYC-LI-CT region, similar recent multi-agency campaigns in the United States include the 2013 Deriving Information on Surface Conditions from Column and Vertically Resolved Observations Relevant to Air Quality (DISCOVER-AQ) Texas campaign;[8] the 2017 Lake Michigan Ozone Study (LMOS);[9] the 2017/2018 Ozone Water–Land Experimental Transition Study (OWLETS) over the Chesapeake Bay;[10] and the 2019 Satellite Coastal and Oceanic Atmospheric Pollution Experiment along the Louisiana Coast (SCOAPE).[11] All these above regions are currently characterized as the critical regions for studying ozone pollution, with a focus on the interplay of urban ozone precursor emissions (NO_x, volatile organic compounds (VOCs)/volatile chemical products (VCPs), *etc.*),[12–15] summertime extreme meteorological conditions (*i.e.*, heatwave days)[16,17] and especially the influence of the sea breeze at coastal regions.[18–23]

The mesoscale sea breeze, most frequently occurring during summertime, is triggered by the thermal contrast between the warmer air over land and the cooler air over water.[24–26] This circulation from the marine boundary layer onto the coastal land area can, at times, return aged polluted air onto the coastal area and degrade the air quality.[27] These polluted plumes can originate directly from the fresh urban emissions, which meet the onshore sea breeze and follow it, or from the nighttime/early morning urban emissions, which are transported to the marine surface by the nighttime/early morning offshore wind, undergo photochemical reactions to form ozone, and back inland following the afternoon development of the sea breeze.[25,27] Besides the above coastal regions in the United States, recent studies of the influence of the sea breeze on the urban high ozone pollution have also been reported at (1) the southern/Mediterranean countries in Europe,[28,29] (2) the Yangtze River Delta of eastern China,[30,31] Hong Kong and Pearl River Delta of southern China,[32] (3) the west coast of Indian,[33] (4) the Seoul metropolitan area of Korea,[34] (5) Boston region of United States,[35] *etc.* For the 2018 LISTOS study, our recent work has highlighted the occurrence of sharp surface ozone heterogeneity over 18 ppb km^{-1} at the Long Island south shore with the maximum ozone concentration over 100 ppb covering a narrow range (around 1 km) of the coastal boundary.[20] The mechanism for this phenomenon is different from the prevalent mechanism for elevated downwind ozone, which suggests pollution precursors from the urban core are transported by a slowly moving southwesterly flow allowing ozone formation and build up over the Long Island north shore and even the whole of Long Island Sound. However, there is limited information about this mechanism for the high ozone over a narrow range of Long Island south shore and the occurrence frequency due to the lack of monitoring sites along the south shore. To make up for this, a new Long Island south shore special monitoring site at Heckscher State Park (HSP, Fig. S1†) was set up in 2021 for collecting relevant air pollutants and meteorological measurements during the ozone season from May to September 2021, 2022, and 2023, to help identify the details of these mechanisms in conjunction with the ozone and meteorological data from the observation networks and a high-resolution model.

2. Methods

2.1 Heckscher State Park monitoring site

The monitoring site is located at Heckscher State Park, close to the shore of Great South Bay (Fig. S1†). Measurements include continuous O_3 from a Teledyne Advanced Pollution Instrumentation (TAPI) T400, NO_2 from a TAPI N500, and meteorological parameters (including Temperature, RH, Pressure, wind speed, and wind direction) from a Lufft weather station at 1 minute temporal resolution through the mid-spring to early fall (May 1 to Sep. 30) from 2021 to 2023. Instruments for measuring ozone and NO_2 were calibrated using a TAPI T700U calibrator, with the ozone generation and NO cylinder standard certified by the Quality Assurance Bureau of the New York State Department of Environmental Conservation. On site QA activities included (1) full multi-point calibrations at the beginning and end of each ozone season, and (2) calibration checks every week during the measurement periods. In addition, EPA standard VOC canister whole air and 2,4-dinitrophenylhydrazine (DNPH) cartridge samples were collected every-6-days, with analysis (following US EPA Method TO-15 and PAMS for whole air and US EPA Method TO-11A for cartridges, respectively) by New York State Department of Environmental Conservation (NYS DEC).

2.2 Other data sources

In this study, the hourly averaged ozone concentration from the NYS DEC monitor sites over the New York metropolitan area were used, including the site at Fresh Kills West (FKW, Staten Island west of NYC urban), City College of New York (CCNY, NYC urban), Queens College (QC, east of NYC urban and west of Long Island), Flax Pond (FP, north shore of Long Island and south of Long Island Sound), Babylon and Suffolk County (BL and SC, middle Long Island), with the locations in Fig. S1† and data from https://www.nyaqinow.net/. Besides the local meteorology captured by the Lufft weather sensor at HSP, the Doppler lidar profiles for the wind direction/speed in a vertical range of 100 m to 2 km with a time resolution of 10 min were utilized from three New York State Mesonet sites at Wantagh (WT, south shore of Long Island), QC (east of NYC urban and west of Long Island, also south–north mid of Long Island), and Stony Brook (SB, north shore of Long Island) (Fig. S1†) (https://www2.nysmesonet.org).[36,37] Additionally, this study used the High-Resolution Rapid Refresh Model (HRRR) simulation with a spatial resolution of 3 km for the meteorology from the University of Utah archive (https://home.chpc.utah.edu/~u0553130/Brian_Blaylock/cgi-bin/hrrr_download.cgi),[38] and the 24 hours back trajectories from the National Oceanic and Atmospheric Administration (NOAA) Hybrid Single-Particle Lagrangian Integrated Trajectory (HYSPLIT) atmospheric transport and dispersion modeling system using the HRRR 3 km resolution meteorological data (https://www.arl.noaa.gov/hysplit/).[39] The HYSPLIT was constructed

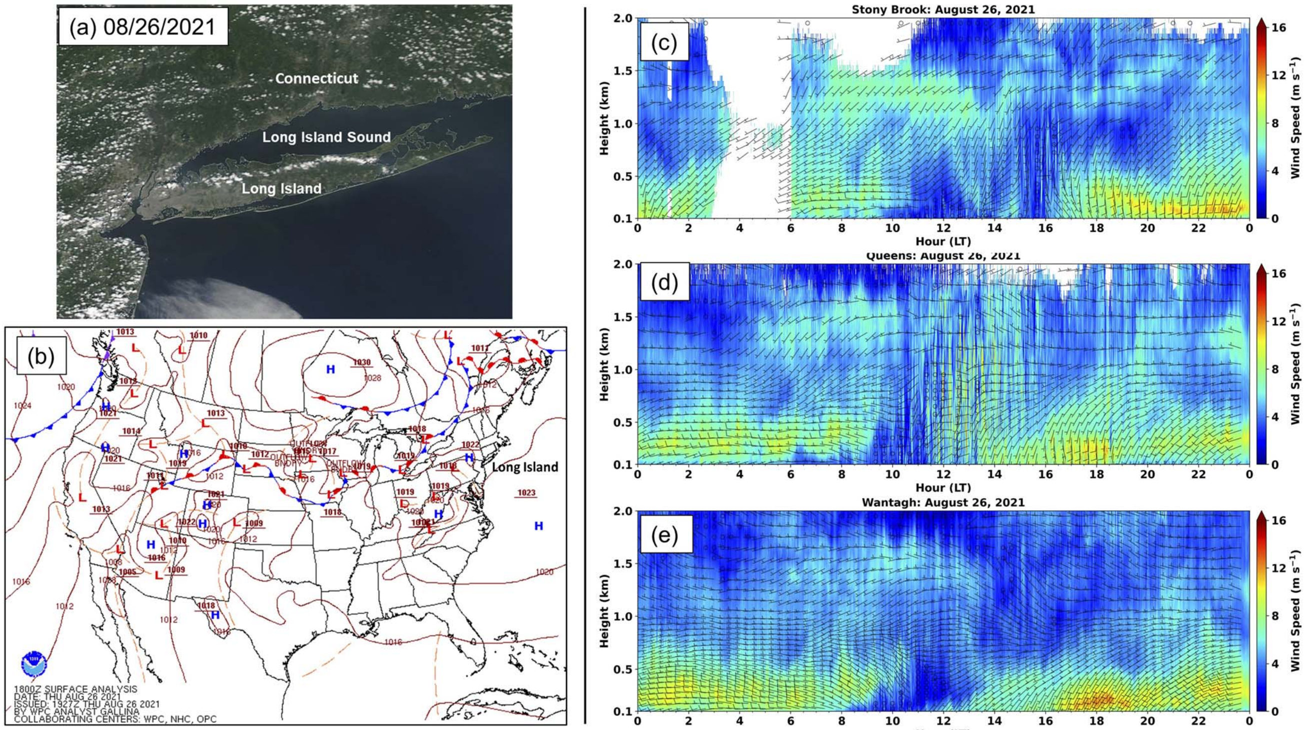

Fig. 1 An example of the multi-platform analyses for the "sea/shore breeze day" identification on 08/26/2021. (a) The EOSDIS Worldview visible satellite imagery (source: https://www.earthdata.nasa.gov/worldview), (b) the Weather Prediction Center surface weather maps for US (14:00 EDT, source: https://www.wpc.ncep.noaa.gov), and (c, d and e) the lidar wind profiles from the Mesonet site in Stony Brook, Queens, and Wantagh.

using HSP (40.70 °N 73.17 °W) as the receptor with three heights of 10 m, 50 m, and 100 m (above ground level).

2.3 Sea/shore breeze days identification

One key aspect of this study was the identification of the occurrence of the southerly sea breeze and northerly shore breeze over Long Island. Here, a manual, multi-platform approach was used as described by Sills *et al.* (2011),[40] Wentworth *et al.* (2015),[41] and Zhang *et al.* (2020),[20] including (1) the visible satellite imagery from the National Aeronautics and Space Administration Earth Observing System Data and Information System (NASA's EOSDIS) Worldview (**https://worldview.earthdata.nasa.gov**), and (2) the Doppler lidar profiles from Wantagh, Queens College, and Stony Brook sites as mentioned above. A day with the simultaneous presence of a sharp gradient in cumulus cloudiness quasi-parallel to the Long Island Sound north coastline in Connecticut state and a line of cumulus clouds parallel to the LI shoreline (Fig. 1a) was identified to be affected by Long Island Sound shore breeze (these two cloud conditions should not be associated with a synoptic front, Fig. 1b). Due to (1) the similar land–sea

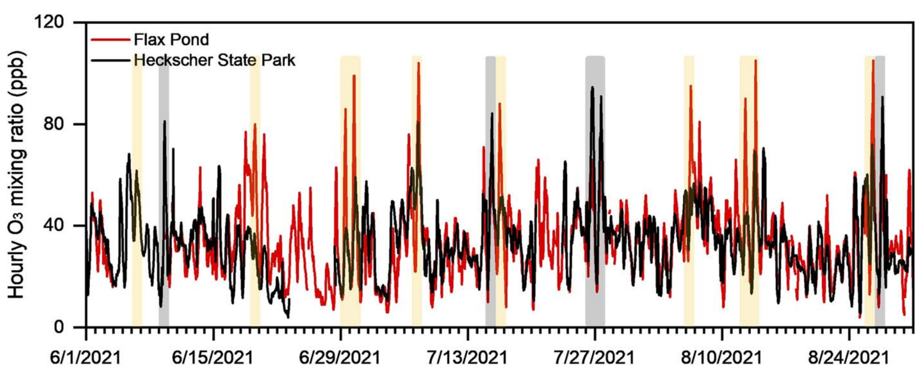

Fig. 2 Hourly averaged O_3 concentration comparison for Flax Pond (FP, north coastal site) and Heckscher State Park (HSP, south coastal site). The grey sections mark high O_3 at HSP, while the yellow sections mark high O_3 at FP. Fig. S1† for the locations of the DEC sites. 06/06 was marked as yellow due to the high O_3 around Long Island Sound (Fig. S2†) even though the data for FP was missing.

conditions over Long Island north and south shore and (2) the distinctive line of cumulus clouds over central Long Island, the day with the northerly Long Island Sound shore breeze over Long Island was also believed to have the southerly sea breeze, as classified as a "sea/shore breeze day". This is further supported by the clear wind variation of the southerlies in the near-surface layer (generally below 1 km) observed from the lidar profiles indicating the sea breeze development with (1) the maximum sea breeze speed occurring around 16:00–18:00 (Eastern Daylight Time, EDT) at Wantagh site and (2) the sea breeze was moving from south (Wantagh site) to north (Stony Brook site, Fig. 1c and d and S2†). It should be noticed that a synoptic front frequently occurred over the north regimes of Long Island (Fig. 1b and S2†), and in these cases produces a westerly synoptic wind (Fig. 1c–e, and S2†), which caused a shift of the southerly sea breeze to southwesterly and promote urban plumes transporting northeasterly from NYC urban regions to the Long Island north shore.

3. Results and discussion

3.1 Case days with coastal high ozone concentrations

Totally fifteen days showed clear ozone spatial heterogeneity between the north *vs.* south coastal sites of Long Island and a maximum hourly O_3 concentration over 80 ppb at one or more of the NYC/Long Island sites (Fig. 2), with ten days had a higher

Table 1 Selected days with clear high ozone and spatial heterogeneity over Long Island (heterog.: the comparison of north *vs.* south shore; temp.: the daily maximum temperature from QC; BH: if affected by Bermuda high with Y for "yes" and N for "no"; Fig. num.: the figure number for the O_3 time series of each day)

	06/06	06/09	06/19	06/29	06/30	07/07	07/15
Heterog.	N > S	S > N	N > S	N > S	N > S	N > S	S > N
Temp.	32.9 °C	31.9 °C	31.6 °C	33.7 °C	34.3 °C	32.8 °C	31.1 °C
BH	Y	Y	Y	Y	Y	Y	Y
Fig. num.	Fig. S6	Fig. S7	Fig. S6	Fig. S6	Fig. S6	Fig. S6	Fig. 4

	07/16	07/26	07/27	08/06	08/26	08/27
Heterog.	N > S	S > N	S > N	N > S	N > S	S > N
Temp.	31.2 °C	31.6 °C	31.2 °C	29.3 °C	33.1 °C	33.8 °C
BH	Y	N	Y	Y	Y	Y
Fig. num.	Fig. S6	Fig. 4	Fig. S7	Fig. S6	Fig. 3	Fig. 4

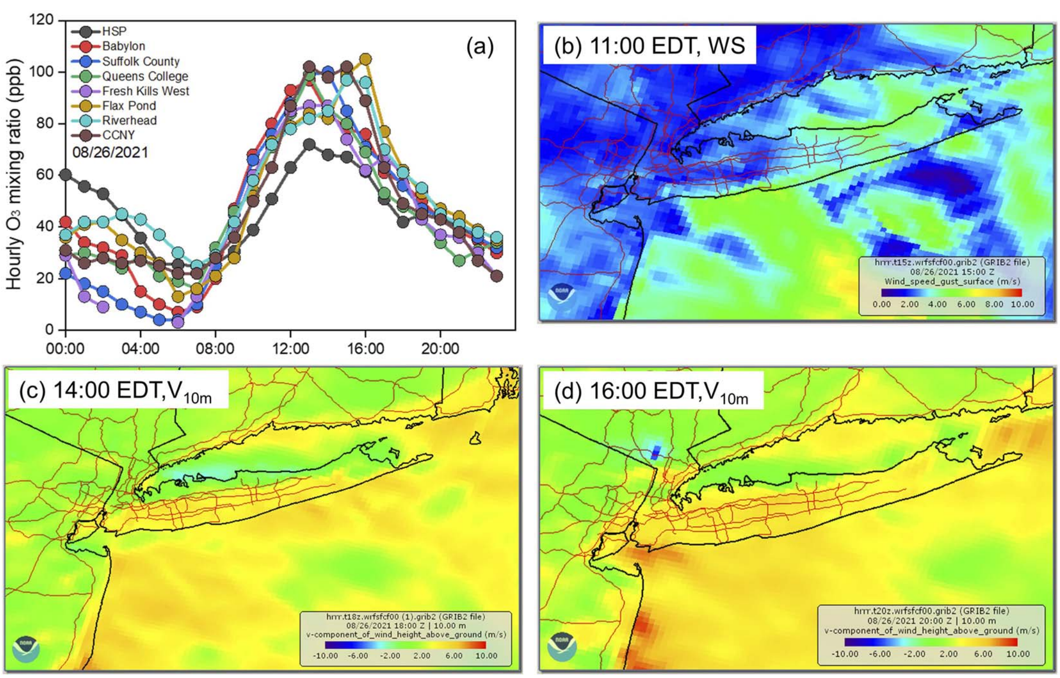

Fig. 3 Plots for 08/26/2021 with north coastal high ozone. (a) The time series of hourly O_3 concentrations for selected DEC sites in NYC and Long Island region; (b) the HRRR ground wind gusts map at 11:00 EDT, (c) the HRRR 10 m wind v-component (south–north direction) speed at 14:00 EDT, and (d) the HRRR 10 m wind v-component (south-north direction) speed at 16:00 EDT.

maximum hourly O_3 concentration at the north site (FP) than the south site (HSP) and the remaining five days had the reverse gradient (Table 1 for the selected thirteen days as mentioned below). They were all marked as hot summer days with the daily maximum temperature near/over 30 °C (temperature data from Queens College (QC) site), and most of them were affected by the Bermuda high (Fig. S2 and S3†), all of which favor O_3 formation and high ground-level concentrations.[42–45] While Bermuda high conditions are known to be associated with high regional O_3, the significant O_3 spatial heterogeneity observed in 2018 highlights the influence of other factors on the O_3 distribution, *i.e.* local sea breeze circulation.[20] Among these ten days with higher O_3 concentration at the north shore, eight were classified as "sea/shore breeze days" (Fig. S2†), matching the LISTOS assumption of high ozone over the Long Island Sound regions being affected by the land–sea circulation (Fig. S4†), and will be discussed in the following section. The five days with the higher O_3 concentration at the south shore were also considered to have sea/sound breeze formation (Fig. S3†), except July 26 when the line of cumulus clouds over Long Island on July 26 was associated with a synoptic stationary front, as discussed in Section 3.3. Considering the existence of the sharp gradient in cumulus cloudiness in Connecticut state and the enhanced southerly wind speed around 16:00 EDT, it is reasonable to infer that the sea/shore breeze may have also occurred on July 26. Meanwhile, the high O_3 mainly clustered in a narrow range over the south coastal line for these five days (Fig. S5†), rather than expanding into a large range or moving to the north side. However, the reasons for this are still not totally clear and could be related to more complex coastal meteorology. Thus, exploring and explaining the complications of coastal meteorology for influencing the high ozone occurrences over Long Island shore, especially for the south shore, is the focus of this study.

3.2 North shore cases: urban plume transported along a sea breeze convergence front

There are a number of common features that occurred on the days with the north coastal high ozone. Refer to Fig. 3a, 8/26/2021 as an example, and find hourly ozone data for the other ten days in Fig. S6.† These common features include: (1) relatively calm conditions over western Long Island (and extending

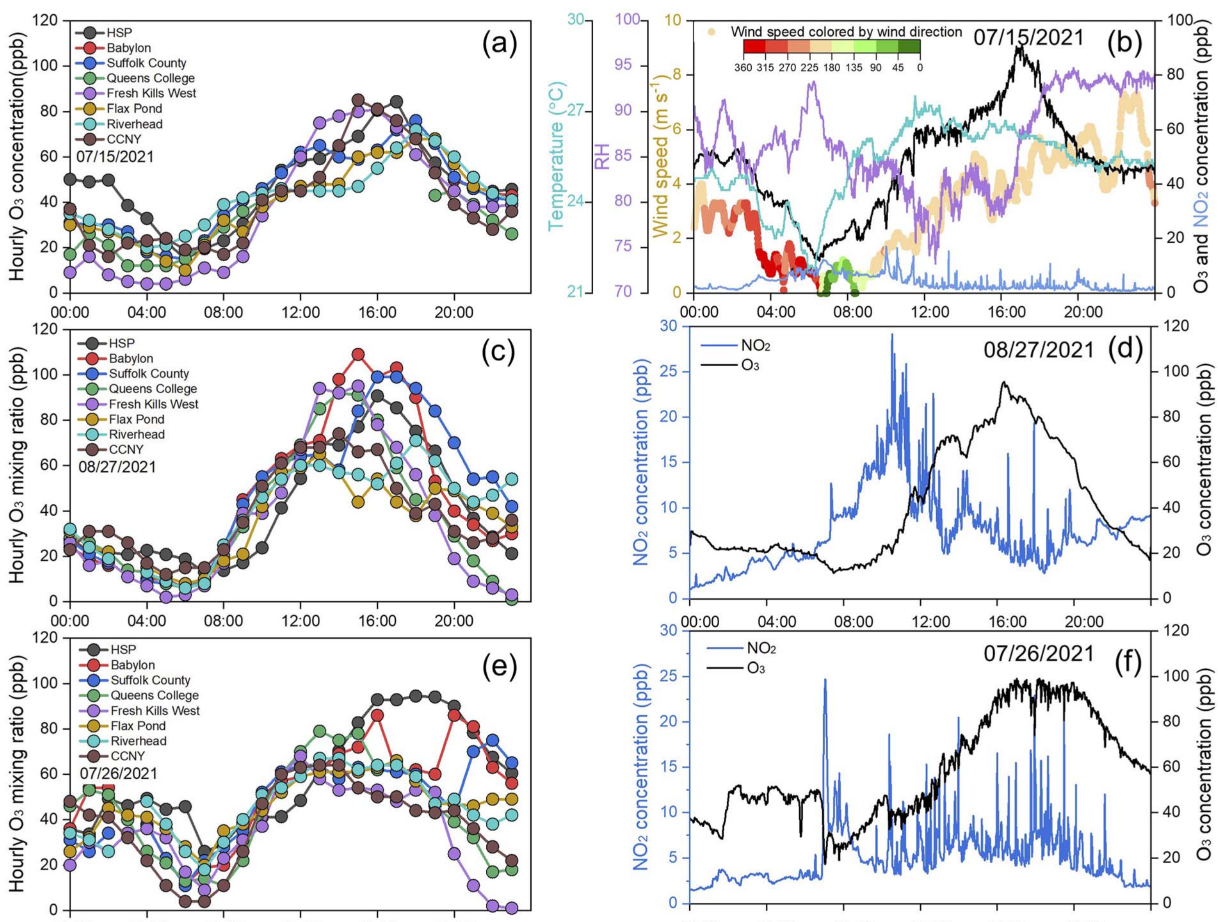

Fig. 4 The time series of (a) the hourly O_3 concentration at the selected DEC sites on 07/15/2021, (b) the minute average O_3 and NO_2 concentrations, RH, and wind speed colored by wind direction at HSP on 07/15/2021, (c) the hourly O_3 concentration at the selected DEC sites on 08/27/2021, (d) the minute average O_3 and NO_2 concentrations at HSP on 08/27/2021, (e) the hourly O_3 concentration at the DEC sites on 07/26/2021 and (f) the minute average O_3 and NO_2 concentrations at HSP on 07/26/2021.

at times into NYC) in the morning (around 10:00–12:00 EDT, Fig. 1c and e from lidar profiles, and Fig. 3b from HRRR simulation); (2) weak, but persistent westerly winds from the NYC/NJ region before the morning calm condition at the QC site, followed by southwesterly sea breeze after the calm around noon (Fig. 1d); (3) an afternoon sea/bay breeze convergence flow along the Long Island north shore and Long Island Sound encompassing the Stony Brook site lasting for about 2 hours (15:00–17:00 EDT), with the wind direction shifting from northerly to southwesterly, indicating a stagnant sea breeze front (Fig. 1c).[33–36] The lidar profiles for all other days with higher ozone on the north side of Long Island are shown in Fig. S2.† There was a 3 hours difference between the sea breeze onset at Wantagh and Stony Brook (12:00 EDT *vs.* 15:00 EDT), reflecting the transit time of the sea breeze front from the south to the north over a distance of about 23 km (Wantagh *vs.* Stony Brook) under a near-ground v-component wind speed of about 8 km h^{-1} (Fig. 1e). More specifically, HRRR results clearly show the movement of the sea breeze front and its related convergence flow through the map of v-component wind speeds (south–north direction, 10 m winds) at different times (14:00 EDT *vs.* 16:00 EDT, Fig. 3c *vs.* Fig. 3d). The line of reasoning is further bolstered by maps showing the line of cumulus cloud from south to north as a result of the breeze front moving (Fig. S8a and S8b†).

Given the low/moderate NO_2 concentration (2.4–4.6 ppb) at Flax Pond during daytime and the high NO_2 concentration covering the west of Long Island under the morning calm conditions (Fig. S8c†), it is reasonable to conclude that the high O_3 at FP was photochemically aged and transported in rather than from local production, and the high O_3 plumes are from the NYC urban region where the freshly emitted NO_2 reacted to form O_3 around noon and/or from the marine surface containing photochemically aged urban plumes, which was transported to the marine surface by nighttime/early morning offshore wind. More detailed plume-tracking measurements could be useful to fill in the details of this mechanism. Similar high O_3 was also shown in the 2018 LITSOS mobile lab on-road measurements near Sands Point at the north shore[20] and by the 2018/2019 Flax Pond ozone sondes measurements[21] over vertical ozone profiles.

3.3 South shore cases: late-afternoon marine winds returning aged urban plumes

For the five days with higher ozone along the Long Island south shore, the timing for peak O_3 was consistently around 16:00–17:00 EDT (HSP in Fig. 4), which may indicate they shared similar high O_3 formation pathways to some extent. However, the difference in the O_3 spatial distributions among these five days, with (1) only high O_3 at HSP on July 15 and 27, (2) high O_3 extending into the middle of Long Island (Babylon and Suffolk County) on June 09 and Aug. 27, and (3) high O_3 plateau lasting for 5 hours at only HSP on July 26, indicates considerable diversity for these cases and will be presented as three subsections.

3.3.1 Interaction of the New York Bight Jet with marine flow returning aged urban plume. The only Long Island site with an hourly maximum ozone concentration over 80 ppb on 07/15/2021 was HSP (Fig. 4a), and the difference between HSP

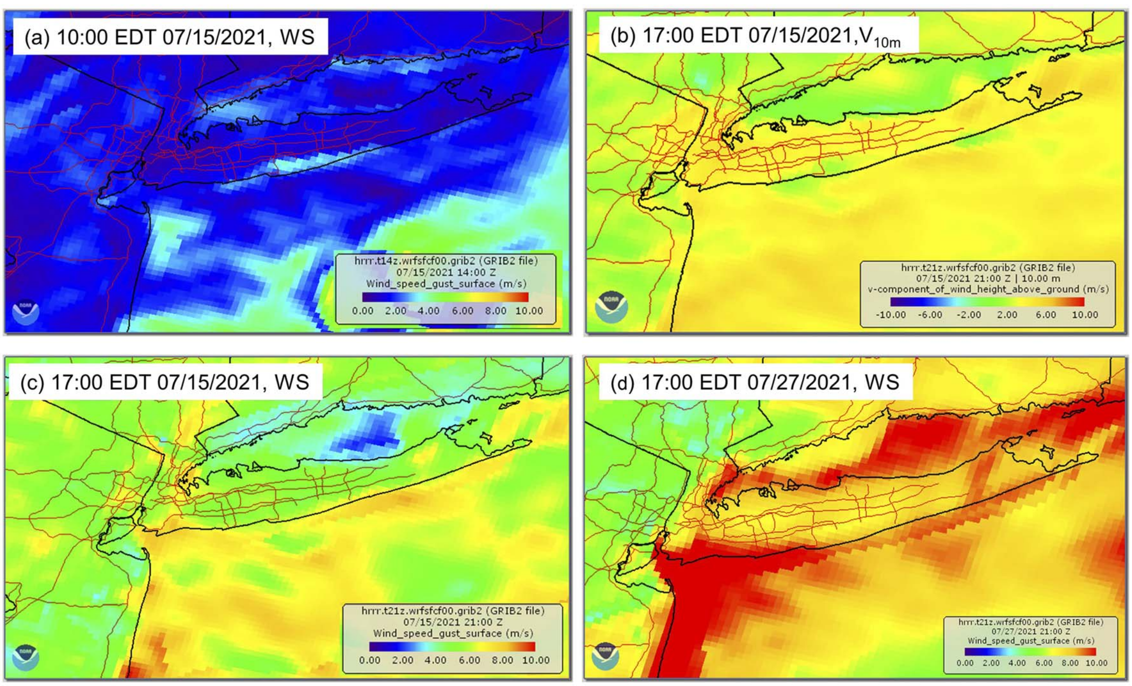

Fig. 5 HRRR wind maps for the days with south coastal high ozone affected by the New York Bight Jet. (a) The HRRR ground wind gust map at 10:00 EDT on 07/15/2021, (b) the HRRR ground wind v-component (south–north direction) speed at 17:00 EDT on 07/15/2021, (c) the HRRR ground wind gust map at 17:00 EDT on 07/15/2021, and (d) the HRRR ground wind gust map at 17:00 EDT on 07/27/2021.

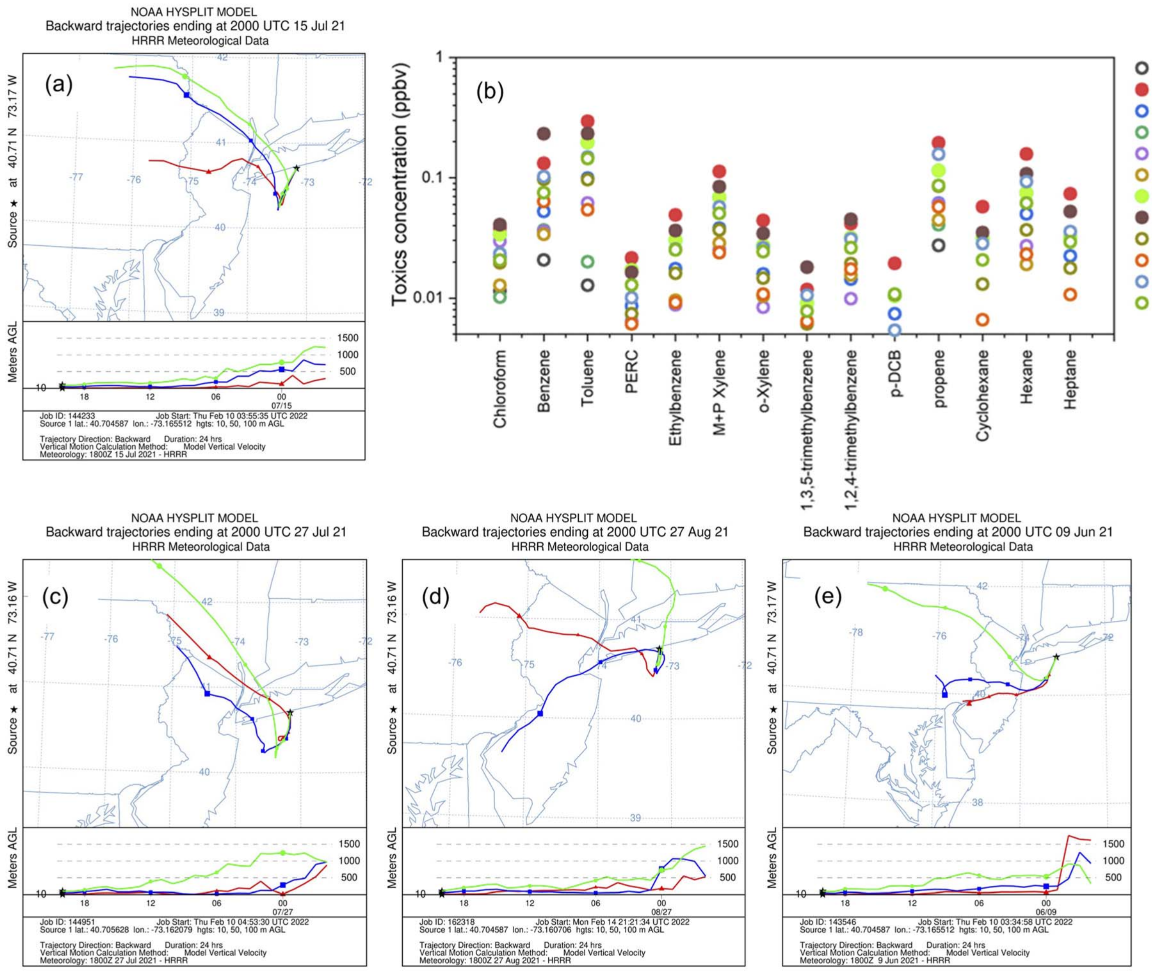

Fig. 6 (a) The HYSPLIT back trajectories with HSP as receptor at 16:00 EDT on 07/15/2021; (b) the carbonyl species concentration (the cases days are solid circles); and (c–e) The HYSPLIT back trajectories with HSP as receptor at 16:00 EDT on 07/27/2021, 08/27/2021, 06/09/2021 (the HYSPLIT back trajectories receptor heights are 10 m (red), 50 m (blue), and 100 m (green). The dates for HYSPLIT back trajectories are sorted following the appearance order in Section 3.3).

(south shore) and FP (north shore) was over 20 ppb. The minute averaged wind data measured from HSP showed low speeds below 1 m s^{-1} around 06:00 EDT (Fig. 4b), matching the start of calm conditions covering the whole NYC metro area as shown in Fig. 5a from the HRRR model simulation and Fig. S3a† from the lidar wind profiles. The calm conditions lasted about 6 hours from around 06:00 EDT to 12:00 EDT, followed by a moderately strong sea breeze front moving from south to north (Fig. S3a and S9†) in the next 5 hours until 17:00 EDT when the front passed over Long Island (Fig. 5b).

Peak O_3 at HSP occurred when the sea breeze front passed the north shore and HSP was dominated by the on-shore southerly wind (around 17:00 EDT). Given the much lower ozone on the north side of Long Island, this case cannot be an example of high O_3 transported along the stagnant sea breeze front as shown for 08/26/2021. In addition, the low NO_2 concentration (Fig. 4b) indicates the O_3 peak was influenced by factors other than local photochemistry. The 17:00 EDT HRRR simulations showed a band with enhanced near-ground southwesterly wind speed (near 8 m s^{-1}, Fig. 5c) with an increased near-ground u-component (west–east direction, 10 m, Fig. S10a†) and slightly reduced near ground v-component (south–north direction, 10 m, Fig. 5b and S10b†). Compared to the near-ground (10 m) layer, u- and v-components both had a distinct enhancement at a higher layer (80 m) (Fig. S10c and d†), implying the presence of the New York Bight Jet (NYBJ).[46,47] The HYSPLIT back trajectory with HSP as the receptor at 17:00 EDT (Fig. 6a) shows that the NJ and NYC urban plume was initially transported to the ocean shallow boundary layer during the nighttime, and was then carried back to Long Island south shore by a southwesterly wet (RH: 88% measured at HSP) and cool (Temp.: 26 °C measured at HSP) marine flow. The enhanced temperature gradient between Long Island and the marine surface during the mid-afternoon (31.1 at °C QC and 22.3 °C at Long Island south Buoy Station 44 025 at 14:00 EDT) contributes to this marine flow formation. This urban-influenced plume that had been over the ocean was also characterized by enhanced anthropogenic related carbonyl species, *i.e.* BTEX (benzene, toluene, ethylbenzene, and xylene), chloroform, *etc.*, as compared to the cleaner "background" days

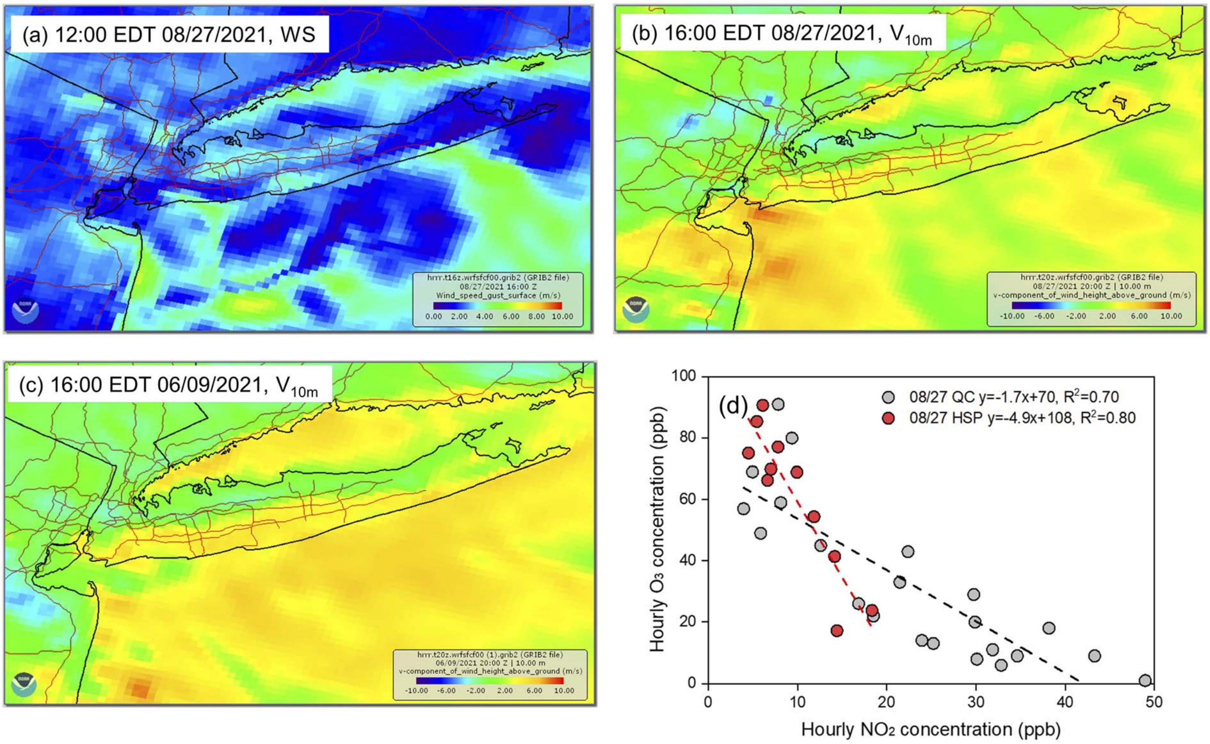

Fig. 7 (a) The HRRR ground wind speed at 12:00 EDT on 08/27/2021; (b) the HRRR ground wind v-component (south–north direction, 10 m) speed at 16:00 EDT on 08/27/2021; (c) the HRRR ground wind v-component (south–north direction, 10 m) speed at 16:00 EDT on 08/27/2021; and (d) hourly O_3 *vs.* NO_2 relationship of QC and HSP on 08/27/2021 (only 09:00 EDT-19:00 EDT was selected for HSP during the photochemically active time period).

(Fig. 6b). Thus, the high ozone formed over the south shore on 07/15/2021 is due to the blockage of that urban-influenced plume by the New York Bight Jet to form a highly polluted band over the south shore.

On 07/27/2021 a similar situation developed, with the formation of a sea breeze (Fig. S3b†) and NYBJ circulations (Fig. 5d), and a return flow of photochemically aged air was observed (Fig. 6c). However, it is notable that although these two cases (07/15 and 07/27) showed similar morning calm conditions over the NYC urban area and an early-afternoon sea breeze front movement from south to north as on 08/26, there was no high ozone at the north shore for these two days. The main reason was attributed to the north-shifted ozone precursors' spatial distribution caused by the weak southerly wind (most likely being an early weak sea breeze) on these two days, rather than the weak westerly wind on 08/26 (Fig. S11†).

3.3.2 Marine return flow urban plumes blocked by the weak sea breeze front. 08/27/2021 was marked by relatively calm conditions over the NYC metro regions (including all of Long Island) and a weak sea breeze developing over Long Island in the afternoon (Fig. 7a and S3c†). The southerly marine breeze was only strong enough to push the front/convergence to the middle of Long Island over Babylon and Suffolk County (Fig. 7b), but not all the way to the north shore (*i.e.*, 08/26 and 07/15, Fig. 3d and 5b). Similar situations were for 06/09/2021 (Fig. 7c and S3d†). Meanwhile, the relatively calm conditions and weak westerly winds promoted NO_2 accumulation over QC (NO_2 as high as 50 ppb, Fig. 7d) and HSP (NO_2 as high as 18.3 ppb, Fig. 7d), which resulted in NO_2–O_3 titration reactions. The $\Delta O_3/\Delta NO_2$ of HSP around noon of 08/27 was −4.9, which was far below the values at QC of −1.7 (Fig. 7d). This provides evidence that high O_3 at HSP is affected more by transport than by local formation. The back trajectories on 08/27 and 06/09 were similar to 07/15 and 07/27 (Fig. 6), in which the NYC urban plume advected over the ocean, aged in sunlit conditions, and was returned to the southern parts of Long Island by a southwesterly marine flow. Thus, the slowly moving (or "weak") breeze front acted to trap the aged urban plumes returned from time spent over the ocean to form high ozone along the south coast.

3.3.3 Marine return flow urban plumes blocked by a synoptic stationary front. The high ozone observed at HSP on 07/26/2021 was the result of a stationary synoptic front, with an hourly O_3 plateau over 90 ppb lasting for 5 hours (Fig. 3e). This O_3 plateau was not observed at most of the other DEC sites over the NYC metro area, except Babylon, which observed high ozone for 3 hours before collapsing. The stationary front covered most of the east coast air-sea boundary from Maine to Maryland and crossed Long Island from west to east (Fig. 8a and b), and was captured by the HRRR model, with weak surface wind and enhanced cloud cover over the front which matched the satellite image (Fig. 8c and d). As shown by the HYSPLIT back trajectories (Fig. S12†), these plumes passed over Baltimore and

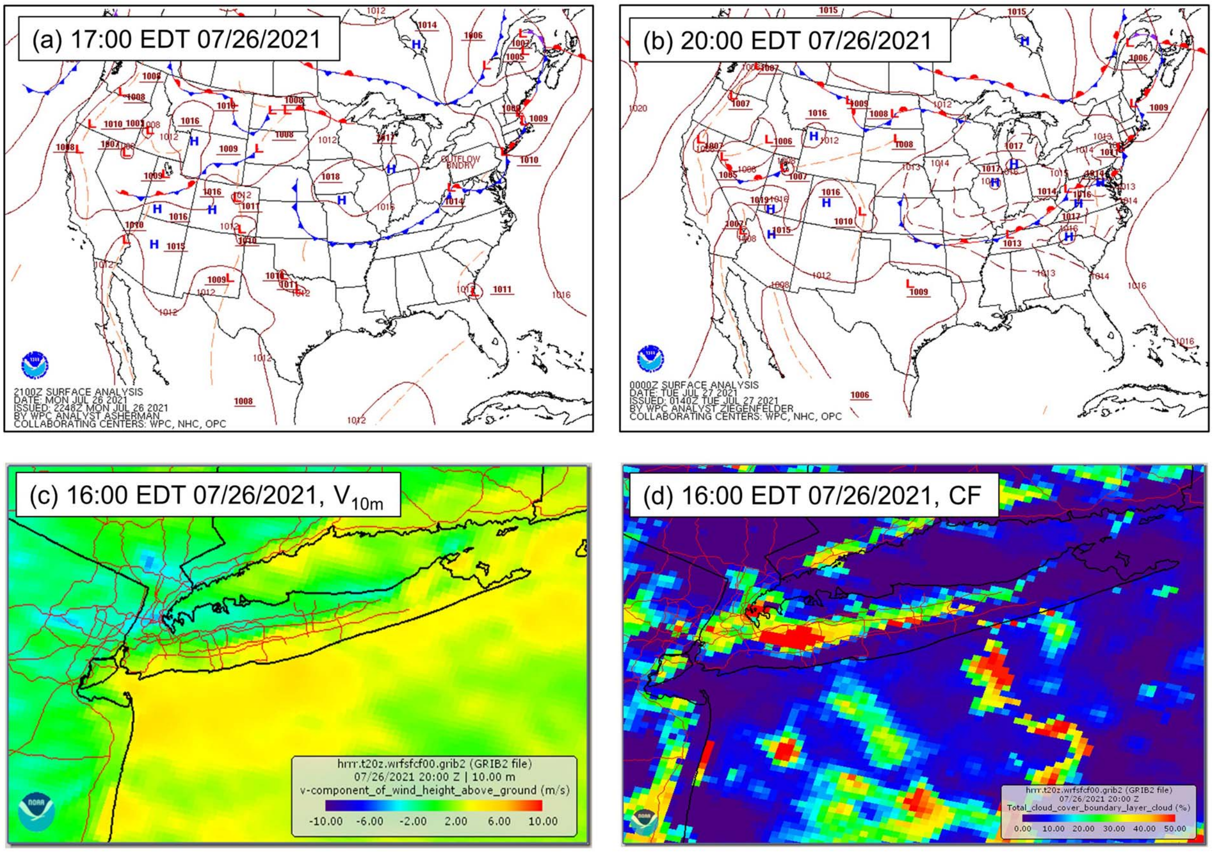

Fig. 8 Plots for 07/26/2021 with south coastal high ozone affected by the synoptic stationary front. (a) The Weather Prediction Center surface weather maps for US at 17:00 EDT; (b) the Weather Prediction Center surface weather maps for US at 17:00 EDT; (c) the HRRR ground wind v-component (south–north direction, 10 m) speed at 16:00 EDT; and (d) the HRRR boundary layer total cloud cover fraction (CF) at 16:00 EDT.

Philadelphia within the Ozone Transport Region to the New York Bight before returning to the Long Island south shore.

Generally similar to the previous studies about the influence of sea breeze affecting the coastal urban regions,[18–35] the processes for producing these types of high O_3 events at the Long Island south shore include: (1) the transport of urban plumes over the ocean south of Long Island, (2) chemical reactions in these polluted plumes to form high ozone in the shallow marine boundary layer, (3) a late-afternoon marine flow carrying this high ozone plume to Long Island. However, the discrepancy comes from the marine flow being blocked by various meteorological conditions (*i.e.*, New York Bight Jet, weak sea breeze front, synoptic stationary front, *etc.*) to form a highly polluted narrow band over the Long Island coastal line, rather than tens of kilometers inland as in previous studies.[19,30] This narrow band just over the coastal line can have serious adverse health effects for people on the coastal beaches, and highlights the necessity for more monitor sites set up along the Long Island south shore. This work also provides important implications for other coastal regions concerning the possible narrow high ozone band quiter near to the coast, and for the need to consider the interplay between the anthropogenic pollutants and the marine environment.[48] Some of these concerns and phenomena are addressed in the upcoming AEROMMA project, in which additional measurements are planned with more instruments to capture the marine chemical signals, including the High-Resolution Time-of-Flight Aerosol Mass Spectrometer (HR-ToF-AMS) for MSA[49] and iodide-ion chemical ionization time-of-flight mass spectrometer (iodide CIMS) for hydroperoxymethyl thioformate (HPMTF).[48]

4. Conclusion

The establishment of the HSP monitoring site on the south shore of Long Island, combined with lidar profiles and HRRR simulations, allows for exploration and for greater understanding of the different mechanisms between the north *vs.* south coastal high ozone. All of the high ozone cases are related to two distinct kinds of urban plumes and their interplay with various marine-related meteorological flows. The cases with higher ozone over the north shore made up the majority of the high ozone days at Long Island, originating from (1) urban plumes from NYC urban regions and their accumulation under the calm conditions caused by the Bermuda high weather pattern to form ozone through photochemical reactions involving NO_x and VOCs, (2) the transport of these high ozone plumes by the early afternoon sea breeze and (3) the accumulation by the stagnant sea breeze front related convergence at the north shore. The contrasting cases involve higher ozone at the south shore and in these cases, the urban plumes were initially transported to the ocean shallow boundary layer during the nighttime/early morning, where efficient ozone formation occurred through photochemical reactions around noon, followed by return transport to the southern Long Island by the late afternoon marine flow. In the cases examined, polluted plumes carried by marine flow were blocked at the south shore by various meteorological conditions (*i.e.*, the New York Bight Jet, the weak sea breeze front, or the synoptic stationary front) to produce high ozone over the south shore for several hours, highlighting the interaction of the anthropogenic pollutants and the marine environment. The good agreement between the HRRR model simulations and the sea breeze front movements is encouraging and offers hope for better simulating the precise location of either north or south shore high O_3, understanding the more detailed O_3 formation and its transportation, and for planning and future emission controls to reduce the occurrence of high O_3 either at the north or south shores of Long Island. These observed coastal (north *vs.* south) O_3 highs and explored formation mechanisms provide practical and valuable guidance to the coming aircraft measurements, including Atmospheric Emissions and Reactions Observed from Megacities to Marine Areas (AEROMMA), the Greater New York (NY) Oxidant, Trace gas, Halogen, and Aerosol Airborne Mission (GOTHAAM), the Coastal Urban Plume Dynamics Study (CUPiDS, https://csl.noaa.gov/projects/aeromma/cupids/), and other related collaborative field campaigns and modeling work, and improve the understanding of the NYC urban plume chemistry and its interaction with coastal meteorology. Meanwhile, this study will also attract additional attention to the high ozone over the south shore by filling the data gap, and inspire similar field campaigns in other world coastal regions affected by the interplay of urban plumes and marine flows.

Conflicts of interest

There are no conflicts of interest to declare.

Acknowledgements

This work has been supported by the Northeast States for Coordinated Air Use Management (NESCAUM) through a contract with the New York State Energy Research and Development Authority (NYSERDA) (Agreement No. 101132) as part of the LISTOS project. Additional funding was provided from NYSERDA Contract 48971. Any opinions expressed in this article do not necessarily reflect those of NYSERDA or the State of New York. We also acknowledge the assistance of many people from the New York State Departments of Environmental Conservation and Parks, Recreation, and Historical Preservation.

References

1 O. Cooper, R. Gao, D. Tarasick, T. Leblanc and C. Sweeney, Long-term ozone trends at rural ozone monitoring sites across the United States, 1990–2010, *J. Geophys. Res.: Atmos.*, 2012, **117**, D22307.

2 I. B. Pollack, T. B. Ryerson, M. Trainer, J. A. Neuman, J. M. Roberts and D. D. Parrish, Trends in ozone, its precursors, and related secondary oxidation products in Los Angeles, California: A synthesis of measurements from 1960 to 2010, *J. Geophys. Res.: Atmos.*, 2013, **118**(11), 5893–5911.

3 B. Hassler, B. C. McDonald, G. J. Frost, A. Borbon, D. C. Carslaw, K. Civerolo, *et al.*, Analysis of long-term observations of NO_x and CO in megacities and application to constraining emissions inventories, *Geophys. Res. Lett.*, 2016, **43**(18), 9920–9930.

4 Z. Jiang, B. C. McDonald, H. Worden, J. R. Worden, K. Miyazaki, Z. Qu, *et al.*, Unexpected slowdown of US pollutant emission reduction in the past decade, *Proc. Natl. Acad. Sci. U. S. A.*, 20182018, **115**, 5099–5104.

5 R. F. Silvern, D. J. Jacob, L. J. Mickley, M. P. Sulprizio, K. R. Travis, E. A. Marais, *et al.*, Using satellite observations of tropospheric NO_2 columns to infer long-term trends in US NO_x emissions: the importance of accounting for the free tropospheric NO_2 background, *Atmos. Chem. Phys.*, 2019, **19**, 8863–8878.

6 EPA, *Our nation's air, 2021*, available at, https://gispub.epa.gov/air/trendsreport/2021/, accessed Feb. 2021.

7 A. Karambelas, *LISTOS: Toward a Better Understanding of New York City's Ozone Pollution Problem*, EM Magazine, 2020.

8 X. Li, Y. Choi, B. Czader, A. Roy, H. Kim, *et al.*, The impact of observation nudging on simulated meteorology and ozone concentrations during DISCOVER-AQ 2013 Texas campaign, *Atmos. Chem. Phys.*, 2016, **16**, 3127–3144.

9 C. O. Stanier, R. B. Pierce, M. Abdi-Oskouei, Z. E. Adelman, J. Al-Saadi, H. D. Alwe, *et al.*, Overview of the Lake Michigan Ozone Study 2017, *Bull. Am. Meteorol. Soc.*, 2021, **102**(12), E2207–E2225.

10 J. T. Sullivan, T. Berkoff, G. Gronoff, T. Knepp, M. Pippin, D. Allen, *et al.*, The Ozone Water–Land Environmental Transition Study: An Innovative Strategy for Understanding Chesapeake Bay Pollution Events, *Bull. Am. Meteorol. Soc.*, 2021, **100**(2), 291–306.

11 A. M. Thompson, D. E. Kollonige, R. M. Stauffer, N. Abuhassan, A. E. Kotsakis, R. J. Swap, *et al.*, *SCOAPE: Satellite and Shipboard Views of Air Quality along the Louisiana Coast*, EM Magazine, 2020, pp. 2470–4741.

12 M. P. Vermeuel, G. A. Novak, H. D. Alwe, D. D. Hughes, R. Kaleel, A. F. Dickens, *et al.*, Sensitivity of Ozone Production to NO_x and VOC Along the Lake Michigan Coastline, *J. Geophys. Res.: Atmos.*, 2019, **124**, 10989–11006.

13 M. M. Coggon, G. I. Gkatzelis, B. C. McDonald, J. B. Gilman, R. H. Schwantes, N. Abuhassan, *et al.*, Volatile chemical product emissions enhance ozone and modulate urban chemistry, *Proc. Natl. Acad. Sci. U. S. A.*, 2021, **118**(32), 1–9.

14 S. Ma, D. Tong, L. Lamsal, J. Wang, X. Zhang, Y. Tang, *et al.*, Improving the predictability of high-ozone episodes through dynamic boundary conditions, emission refresh and chemical data assimilation during the Long Island Sound Tropospheric Ozone Study (LISTOS) field campaign, *Atmos. Chem. Phys.*, 2021, **21**, 16531–16553.

15 G. I. Gkatzelis, M. M. Coggon, B. C. McDonald, J. Peischl, J. B. Gilman, K. C. Aikin, *et al.*, Observations confirm that volatile chemical products are a major source of petrochemical emissions in US cities, *Environ. Sci. Technol.*, 2021, **55**, 4332–4343.

16 F. Moshary, A. D. Fortich, Y. Wu, M. Arend, P. Ramamurhty and B. Gross, Observation of fast tropospheric dynamics and impacts on humidity and air pollution during a heatwave event in New York City, as observed by lidars, other profilers and surface measurements, *Proceedings of the 29th International Laser Radar ConferenceEPJ Web of Conferences*, 2020, vol. 237, p. 03018.

17 J. Zhang, J. Mak, Z. Wei, C. Cao, M. Ninneman, J. Marto and J. J. Schwab, Long Island enhanced aerosol event during 2018 LISTOS: Association with heatwave and marine influences, *Environ. Pollut.*, 2021, **270**, 116299.

18 C. P. Loughner, M. Tzortziou, M. Follette-Cook, K. E. Pickering, D. Goldberg, C. Satam, *et al.*, Impact of bay-breeze circulations on surface air quality and boundary layer export, *J. Appl. Meteorol. Climatol.*, 2014, **53**(7), 1697–1713.

19 V. Caicedo, B. Rappenglueck, G. Cuchiara, J. Flynn, R. Ferrare, A. J. Scarino, *et al.*, Bay breeze and sea breeze circulation impacts on the planetary boundary layer and air quality from an observed and modeled DISCOVER-AQ Texas case study, *J. Geophys. Res.: Atmos.*, 2019, **124**(13), 7359–7378.

20 J. Zhang, M. Ninneman, E. Joseph, M. J. Schwab, B. Shrestha and J. J. Schwab, Mobile Laboratory Measurements of High Surface Ozone Levels and Spatial Heterogeneity During LISTOS 2018: Evidence for Sea Breeze Influence, *J. Geophys. Res.: Atmos.*, 2020, **124**, e2019JD031961.

21 V. Caicedo, R. Delgado, W. T. Luke, X. Ren, P. Kelley, P. R. Stratton, *et al.*, Observations of bay-breeze and ozone events over a marine site during the OWLETS-2 campaign, *Atmos. Environ.*, 20212021, **263**, 118669.

22 M. H. Couillard, M. J. Schwab, J. J. Schwab, C. H. Lu, E. Joseph, B. Stutsrim, *et al.*, Vertical Profiles of Ozone Concentrations in the Lower Troposphere Downwind of New York City during LISTOS 2018–2019, *J. Geophys. Res.: Atmos.*, 2021, **126**, e2021JD035108.

23 A. Torres-Vazquez, J. Pleim, R. Gilliam and G. Pouliot, Performance Evaluation of the Meteorology and Air Quality Conditions from Multiscale WRF-CMAQ Simulations for the Long Island Sound Tropospheric Ozone Study (LISTOS), *J. Geophys. Res.: Atmos.*, 2022, e2021JD035890.

24 R. S. Gaza, Mesoscale meteorology and high ozone in the northeast United States, *J. Appl. Meteorol.*, 1998, **37**(9), 961–977.

25 S. T. K. Miller, B. D. Keim, R. W. Talbot and H. Mao, A review of the sea breeze, *Rev. Geophys.*, 2003, **41**(3), 1011.

26 R. M. Banta, C. J. Senff, J. Nielsen-Gammon, L. S. Darby, T. B. Ryerson and R. J. Alvarez, A bad air day in Houston, *Bull. Am. Meteorol. Soc.*, 2005, **86**(5), 657–670.

27 D. K. Martins, R. M. Stauffer, A. M. Thompson, T. N. Knepp and M. Pippin, Surface ozone at a coastal suburban site in 2009 and 2010: Relationships to chemical and meteorological processes, *J. Geophys. Res.: Atmos.*, 2012, **117**(D5), 1–16.

28 S. Finardi, G. Agrillo, R. Baraldi, G. Calori, P. Carlucci, P. Ciccioli, *et al.*, Atmospheric dynamics and ozone cycle during sea breeze in a Mediterranean complex urbanized coastal site, *J. Appl. Meteorol. Climatol.*, 2018, **57**(5), 1083–1099.

29 M. T. Pay, G. Gangoiti, M. Guevara, S. Napelenok, X. Querol, O. Jorba, *et al.*, Ozone source apportionment during peak summer events over southwestern Europe, *Atmos. Chem. Phys.*, 2019, **19**, 5467–5494.

30 J. Xu, X. Huang, N. Wang, Y. Li and A. Ding, Understanding ozone pollution in the Yangtze River Delta of eastern China from the perspective of diurnal cycles, *Environ. Sci. Technol.*, 2021, **752**, 141928.

31 D. Zhao, J. Xin, W. Wang, D. Jia, Z. Wang, H. Xiao, *et al.*, Effects of the sea–land breeze on coastal ozone pollution in the Yangtze River Delta, China, *Environ. Sci. Technol.*, 2022, **807**, 150306.

32 H. Wang, X. Lyu, H. Guo, Y. Wang, S. Zou, Z. Ling, *et al.*, Ozone pollution around a coastal region of South China Sea: interaction between marine and continental air, *Atmos. Chem. Phys.*, 2018, **18**, 4277–4295.

33 I. A. Girach, N. Ojha and S. S. Babu, Ozone chemistry and dynamics at a tropical coastal site impacted by the COVID-19 lockdown, *J. Earth Syst. Sci.*, 2021, **130**(3), 1–8.

34 Y. H. Ryu, J. J. Baik, K. H. Kwak, S. Kim and N. Moon, Impacts of urban land-surface forcing on ozone air quality in the Seoul metropolitan area, *Atmos. Chem. Phys.*, 2013, **13**(4), 2177–2194.

35 J. A. Geddes, B. Wang and D. Li, Ozone and nitrogen dioxide pollution in a coastal urban environment: The role of sea breezes, and implications of their representation for remote sensing of local air quality, *J. Geophys. Res.: Atmos.*, 2021, **126**(18), e2021JD035314.

36 J. A. Brotzge, J. Wang, C. D. Thorncroft, E. Joseph, N. Bain, N. Bassill, *et al.*, A technical overview of the new york state mesonet standard network, *J. Atmos. Ocean. Technol.*, 2020, **37**(10), 1827–1845.

37 B. Shrestha, J. A. Brotzge, J. Wang, N. Bain, C. D. Thorncroft, E. Joseph, *et al.*, Overview and Applications of the New York State Mesonet Profiler Network, *J. Appl. Meteorol. Climatol.*, 2021, **60**(11), 1591–1611.

38 B. K. Blaylock, J. D. Horel and S. T. Liston, Cloud archiving and data mining of High-Resolution Rapid Refresh forecast model output, *Comput. Geosci.*, 2017, **109**, 43–50.

39 A. F. Stein, R. R. Draxler, G. D. Rolph, B. J. Stunder, M. D. Cohen and F. Ngan, NOAA's HYSPLIT atmospheric transport and dispersion modeling system, *Bull. Am. Meteorol. Soc.*, 2015, **96**(12), 2059–2077.

40 D. M. L. Sills, J. R. Brook, I. Levy, P. A. Makar, J. Zhang and P. A. Taylor, Lake breezes in the southern Great Lakes region and their influence during BAQS-Met 2007, *Atmos. Chem. Phys.*, 2011, **11**, 7955–7973.

41 G. R. Wentworth, J. G. Murphy and D. M. Sills, Impact of lake breezes on ozone and nitrogen oxides in the Greater Toronto area, *Atmos. Environ.*, 2015, **109**, 52–60.

42 J. L. Schnell and M. J. Prather, Co-occurrence of extremes in surface ozone, particulate matter, and temperature over eastern North America, *Proc. Natl. Acad. Sci. U. S. A.*, 2017, **114**(11), 2854–2859.
43 J. Zhu and X. Z. Liang, Impacts of the Bermuda high on regional climate and ozone over the United States, *J. Clim.*, 2013, **26**(3), 1018–1032.
44 J. Hegarty, H. Mao and R. Talbot, Synoptic controls on summertime surface ozone in the northeastern United States, *J. Geophys. Res.: Atmos.*, 2007, **112**(D14), 1–12.
45 L. Shen L, L. J. Mickley and A. P. K. Tai, Influence of synoptic patterns on surface ozone variability over the eastern United States from 1980 to 2012, *Atmos. Chem. Phys.*, 2015, **15**(19), 10925–10938.
46 B. A. Colle and D. R. Novak, The New York Bight Jet: climatology and dynamical evolution, *Mon. Weather Rev.*, 2010, **138**(6), 2385–2404.
47 B. A. Colle, M. J. Sienkiewicz, C. Archer, D. Veron, F. Veron, W. Kempton and J. E. Mak, Improving the Mapping and Prediction of Offshore Wind Resources (IMPOWR): Experimental overview and first results, *Bull. Am. Meteorol. Soc.*, 2016, **97**(8), 1377–1390.
48 P. R. Veres, J. A. Neuman, T. H. Bertram, E. Assaf, G. M. Wolfe, C. J. Williamson, *et al.*, Global airborne sampling reveals a previously unobserved dimethyl sulfide oxidation mechanism in the marine atmosphere, *Proc. Natl. Acad. Sci. U. S. A.*, 2020, **117**(9), 4505–4510.
49 S. Huang, L. Poulain, D. van Pinxteren, M. van Pinxteren, Z. Wu, H. Herrmann and A. Wiedensohler, Latitudinal and seasonal distribution of particulate MSA over the Atlantic using a validated quantification method with HR-ToF-AMS, *Environ. Sci. Technol.*, 2017, **51**(1), 418–426.

